TASK QUARTERLY 12 No 3, 289–301

FAST ALGORITHMS FOR CALCULATIONS OF VISCOUS INCOMPRESSIBLE FLOWS USING THE VELOCITY CORRECTION METHOD

ZBIGNIEW KOSMA AND PRZEMYSŁAW MOTYL

Institute of Applied Mechanics, Technical University of Radom,
Krasickiego 54, 26-600 Radom, Poland
{zbigniew.kosma, p.motyl}@pr.radom.pl

(Received 29 April 2008)

Abstract: The velocity correction method is designed to simulate stationary and non-stationary, two- and three-dimensional motions of a viscous incompressible fluid. The basic assumption of this method consists in splitting the velocity and the pressure fields and calculations are performed in two steps. In the first step, a tentative velocity field is determined by simplified equations for momentum conservation. In the second step the Neumann problem for the Poisson equations is solved to obtain the computational pressure, and the velocity components are corrected. A standard method of lines approach and the two grids method are applied in this contribution. Some test calculations for laminar and transitional flows in square and cubic cavities with one moving wall as well as in a backward-facing step are reported.

Keywords: Navier-Stokes equation, velocity correction method, method of lines, two grids method

1. Introduction

Many realistic problems in low-speed aerodynamics and hydrodynamics can be addressed by incompressible NS equations. The accuracy and efficiency of the existing codes are now such that Computational Fluid Dynamics (CFD) is routinely used in the analysis and improvement process of the existing designs and it is a valuable tool in experimental programs and in the construction of new configurations. However, the CPU requirements for steady and unsteady computations are still very high even with the use of the most powerful super-computers.

The projection methods, proposed by Chorin [1] and Temam [2], are popular techniques for simulating incompressible flows, and many efforts have been made in the simulation of viscous flows by resolving the NS equations with this method and its variants, see *e.g.* [3–56]. This is due to their simple description of the flow in terms of primitive variables, such as velocities and pressure and their algorithmic simplicity. Decoupling the pressure and velocity reduces the problem to the solution of a sequence of simpler problems. With this method, some auxiliary velocity field is found and the

projection into a divergence-free space via the solution of a Poisson equation for some form of the pressure is performed. Some different techniques applied lead to a large variety of schemes, all of which have been occurring in practice for years. Although they require the solution of an elliptic Poisson equation, they are computationally efficient due to the recent advances in linear algebra, such as the incorporation of advanced multigrid methods. It is already linearization or extrapolation of the advection term in time that give some satisfactory results. However, at the same time, they lead to smaller time steps owing to the inherently more explicit character and often suffer from spurious pressure boundary layers. Theoretical considerations can provide some ideas concerning the stability of these schemes, but a complete analysis or a quantitative prediction is not satisfactory today. Therefore, the only way to make a judgement is to perform numerical tests, at least for some classes of problems which seem to be representative.

The proposed new version of the velocity correction method can be considered to be a variation of the projection scheme originally proposed by Huser and Biringen [9]. To overcome the difficulties associated with the nonlinearity of advection terms in the first stage of the calculation, the initial-boundary value problem for the system of partial differential equations is reduced to an initial value problem for a system of ordinary differential equations in the unknown values of tentative velocity components in each inner knot of uniform computational meshes. All the derivatives with respect to the spatial independent variables are approximated by means of the second-order finite-difference schemes, while the continuity of the time-variable is preserved. The resulting system of ordinary differential equations is integrated by using the Heun's method of second order. For solving the Neumann problem for the computational pressure the finite difference method together with the Gauss-Seidel method are applied. The numerical experiments have shown that the computational pressure does not have to be determined accurately, moreover the two grids method has been found to work very well at a reasonably accelerating rate of convergence. To simplify our analysis, this study focuses only on the frequently studied standard benchmark problems to validate the NS solvers accuracy because many approved experimental and numerical results are reported in the literature.

2. Governing equations

The non-dimensionalized governing equations in the Cartesian co-ordinate system become:

$$\left.\begin{aligned} \frac{\partial V_j}{\partial x_j} &= 0, \\ \frac{\partial V_i}{\partial t} + \frac{\partial}{\partial x_j} V_i V_j &= -\frac{\partial p}{\partial x_i} + \frac{1}{\mathrm{Re}} \frac{\partial}{\partial x_j} \frac{\partial}{\partial x_j} V_i, \end{aligned}\right\} \tag{1}$$

where V_1, V_2, V_3 are the velocity components, p is the pressure, and Re is the Reynolds number.

The physical boundary conditions for the equations of viscous flows (1) in primitive variables are specified as consisting of the impermeability and non-slip conditions at the solid walls, and of the assumed velocity profiles requirement at the channel inlet and outlet. The pressure is usually not given on the boundaries, but

it can be obtained from the momentum equations, and can be fixed in one point of the domain.

In the first stage of a modified version of the velocity correction method, the initial-boundary value problem for the intermediate velocity components $\tilde{V}_i = \tilde{V}(x_i,t)$ is solved during the intermediate time step from t^n to $\tilde{t}$, which is determined by the simplified Navier-Stokes equations (2) for the known computational pressure $\tilde{p}^n = \tilde{p}(x_i,t^n)$:

$$\frac{\partial \tilde{V}_i}{\partial t} + \frac{\partial}{\partial x_j}\tilde{V}_i\,\tilde{V}_j = -\frac{\partial \tilde{p}^n}{\partial x_i} + \frac{1}{\mathrm{Re}}\frac{\partial}{\partial x_j}\frac{\partial}{\partial x_j}\tilde{V}_i\,. \tag{2}$$

The Equations (2) are to be solved subject to the initial and boundary conditions taken from the assumption that, the intermediate velocity components $\tilde{V}_i$ on the boundaries $\partial\Omega$ and at the time level $t = t^n$, are equal to the physical velocity components V_i:

$$\tilde{V}_i\big|_{\partial\Omega} = V_i\big|_{\partial\Omega}\,, \quad \tilde{V}_i^n = V_i^n\,. \tag{3}$$

In the second stage at every time step $\Delta t = t_{n+1} - t_n$ for the time step from $\tilde{t}$ to t^{n+1} the velocity components V_i are corrected using the formulas:

$$V_i^{n+1} = \tilde{V}_i - \frac{\Delta t}{2}\left(\frac{\partial \tilde{p}^{n+1}}{\partial x_i} - \frac{\partial \tilde{p}^n}{\partial x_i}\right), \tag{4}$$

adapted after the integration of the equations coupling the velocity fields with the derivatives of computational pressure:

$$\frac{\partial V_i}{\partial t} = \frac{\partial \tilde{V}_i}{\partial t} - \frac{1}{2}\left(\frac{\partial \tilde{p}^{n+1}}{\partial x} - \frac{\partial \tilde{p}^n}{\partial x}\right). \tag{5}$$

Now, applying the discrete divergence to (4) and making use of the first equation from the equation system (1), one can obtain the discrete Poisson equation for the computational pressure $\tilde{p}$ at the time level t^{n+1}:

$$\frac{\partial}{\partial x_j}\frac{\partial}{\partial x_j}\tilde{p}^{n+1} = \frac{\partial}{\partial x_j}\frac{\partial}{\partial x_j}\tilde{p}^n + \frac{2}{\Delta t}\frac{\partial \tilde{V}_j}{\partial x_j}, \tag{6}$$

subject to the Neumann boundary conditions:

$$\left.\frac{\partial \tilde{p}^{n+1}}{\partial \vec{n}}\right|_{\partial\Omega} = 0 \tag{7}$$

at all boundaries – resulting from relationships (3) provided that $\partial\tilde{p}/\partial\vec{n}$ vanishes at the first time step, where $\vec{n}$ is a vector normal to the boundaries.

3. Numerical approach

The proposed numerical technique in the first step of the calculation, the method of lines, consists of converting the initial-boundary value problem (2)–(3) into an ordinary differential equation initial value problem. All the spatial derivatives together with the boundary conditions for the first derivative of pressure are approximated by means of classical, central and one-sided, finite difference approximations

of second order [57]. This produces a system of ordinary differential equations which can be written in the general form:

$$\frac{d\tilde{U}}{dt} = F\big(\tilde{U}\big), \tag{8}$$

where $\tilde{U} = \big[\tilde{V}_i\big]^T$ is the vector of dependent variables, and F is a spatial differential operator.

The unknown values of auxiliary velocity components in each inner knot of computational meshes are computed using the explicit Runge-Kutta method of second order [57]:

$$\tilde{U}_{n+1} = \tilde{U}_n + \frac{\Delta t}{2}\big(K_1 + K_2\big), \tag{9}$$

where $K_1 = F\big(\tilde{U}_n\big)$, $K_2 = F\big(\tilde{U}_n + \Delta t K_1\big)$.

In the second step of the calculation very rapid convergence to a solution of the discretized boundary value problem (6)–(7) is achieved with the aid of a multigrid procedure. The idea behind the multigrid strategy is to accelerate the evolution of the system of equations on the fine grid by introducing auxiliary calculations on a series of a coarser grid. The coarser grid calculations introduce larger scales and larger time steps with the result that low-frequency error components may be efficiently and rapidly damped out. Auxiliary grids are introduced by doubling the grid spacing, and computational pressure values are transferred to a coarser grid. The most convenient and often very effective smoothing process is the iteration due to Gauss and Seidel.

Successful multigrid procedures rely heavily on consistent practices for the construction of the coarse grid equations and for the restriction and prolongation operators. In our calculations a two-grid method has proved to be the most useful. It is described as follows:

- after a few ν_1 iterations on the fine grid, the residuals R_h of the Equation (6) are computed,
- the residuals R_h are restricted to the coarse grid $R_{2h} = I_h^{2h}(R_h)$ (I_h^{2h} is a restriction operator which maps h-grid functions into $2h$-grid functions) and the problem $\Delta e_{2h} = R_{2h}$ is solved with ν_2 fixed number iterations,
- the solution corrections e_{2h} are interpolated from the coarse to the fine mesh $e_h = I_{2h}^h(e_{2h})$ (I_{2h}^h is an interpolation operator). The solution on the finest grid is updated and the problem (6) is solved with additional ν_3 iterations.

4. Numerical simulations

In this section three well-known benchmark flow examples are presented: the driven square [58–83] and cubic cavity flows [66, 84–95] as well as a backward-facing step problem [96–109], which have been widely used to verify codes validation. The streamlines and comparisons between the results of the presented algorithms and those documented in the literature are shown.

4.1. Square and cubic cavity problems

Let us first consider two- and three-dimensional driven cavity flows as drawn in Figure 1 as examples of the developed method. Driven cavity flows are strongly nonlinear for high Reynolds numbers, and in no other class of flows are the boundary

conditions so unambiguous. The wide popularity of these test problems can be attributed to the existence of a variety of the fluid flow phenomena that can possibly occur in incompressible flows: eddies, secondary flows, complex 3D flow patterns. There are a number of industrial contexts in which these flows and the structures that they exhibit play a role.

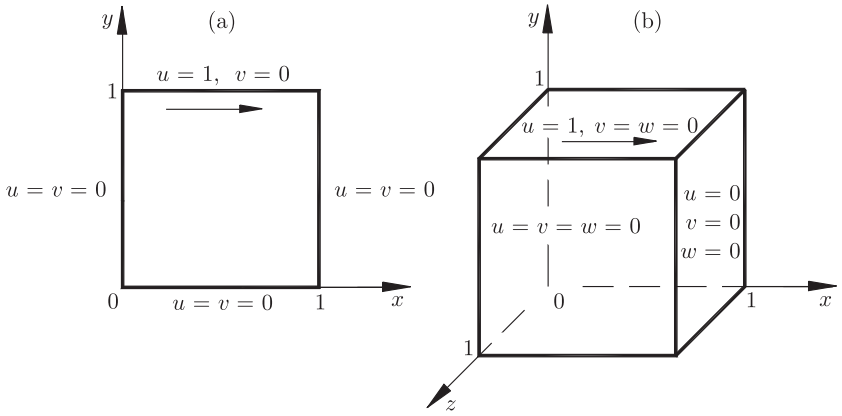

Figure 1. Geometry and boundary conditions of driven cavity problems: (a) square cavity flow, (b) cubic cavity flow

The quadratic domain in the $x-y$ plane (Figure 1a) is first covered by a grid system $N\times N$ defined by:

$$(x_i)_j = jh \quad (j=0,\ 1,\ \ldots,\ N) \tag{10}$$

with constant mesh spacing $h=1/N$.

The spatial discretization is afterwards done on a stretched mesh $N\times N$. The stretching is computed by the formula:

$$x_i = a\xi_i^3 + b\xi_i^2 + c\xi_i \quad (0\le\xi_i\le 1). \tag{11}$$

The coefficients a, b, and c are determined by parameters d_0 and d_N to provide grid points control:

$$a = d_0 + d_N - 2, \quad b = 1 - a - d_0, \quad c = d_0. \tag{12}$$

The grid in the $\xi_1-\xi_2$ plane is uniform. The values of the parameters $d_0<1$ and $d_N<1$ effectively provide the slope of the points distribution in the x_1-x_2 plane so that grid points are clustered close to the cavity boundaries to resolve the high gradients expected in those areas. A simple choice: $d_0=d_N=1$ gives the uniform grid (10).

The computations in the square cavity were first performed for the Reynolds numbers $\mathrm{Re}=100$ and $\mathrm{Re}=400$ on the uniform grid 100×100 with the time step $\Delta t=10^{-2}$, the integration of the system of equations (8) was terminated after arriving at the steady state, defined as:

$$\left\|\dot{\tilde{U}}^{n+1} - \dot{\tilde{U}}^{n}\right\| \le \varepsilon = 10^{-12}. \tag{13}$$

In order to justify the use of the grids number, the computational cost (CPU time) required for computing an approximate solution with the given accuracy (13)

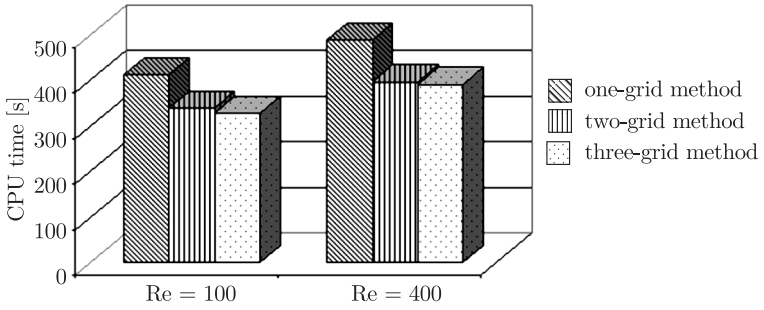

Figure 2. Square cavity comparisons of CPU times for a multigrid method with different number grids, $\mathrm{Re} = 100$ and $\mathrm{Re} = 400$, 100×100 grid

has been investigated. For efficient implementation of multigrid methods, we further assume that $\nu_1 = \nu_3 = 5$, $10 \leq \nu_2 \leq 20$. With these small counts of iterations, the two-grid method is particularly attractive due to its improved convergence rate and takes approximately the same amount of time for computations as the three-grid method (Figure 2). It is not surprising as the number of arithmetic operations in the three-grid method is bigger than that in the two-grid method. However, the three-grid method is shown to have a better smoothing effect of computational errors than the two-grid method (Figure 3).

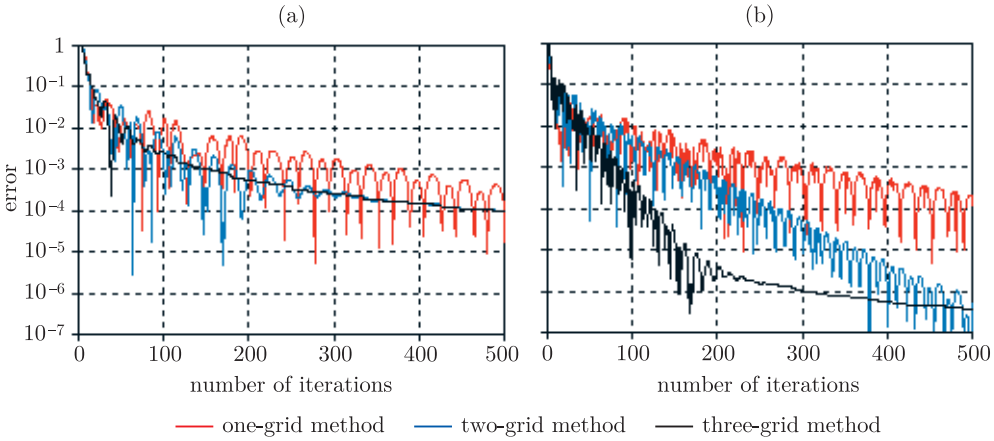

Figure 3. Square cavity – comparisons of calculation errors for a multigrid method with different number grids at $\mathrm{Re} = 100$ on 100×100 grid: (a) velocity components, (b) computational pressure

By using the two-grid method, computations were undertaken on 200×200 and 300×300 uniform grids as well as on 100×100 and 150×150 nonuniform grids. The following slope parameter values (12) were selected:

$$d_0 = d_N = 0.5,\ 0.3,\ 0.15\,. \tag{14}$$

Numerical solutions were done with the time steps taken as $\Delta t = 10^{-3}$ and the same criterion (13) for convergence as previously. Figure 4 shows the plots of velocity components profiles corresponding to the Reynolds number $\mathrm{Re} = 7500$ on a 100×100 nonuniform grid and their comparison to the results reported in [58]. In order to illustrate the use of our fast solver, the obtained stream functions contours

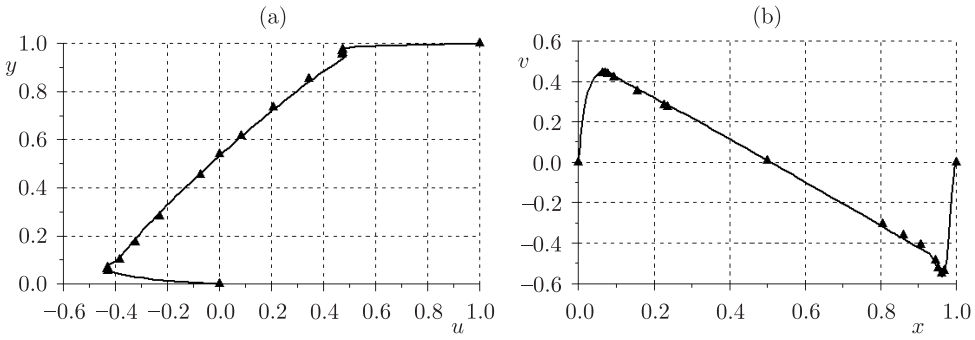

Figure 4. Square cavity – distributions of velocity components at $\mathrm{Re} = 7500$ on 100×100 grid with $d_0 = d_N = 0.3$: (a) u-velocity component on the vertical centerline, $x = 0.5$, (b) v-velocity component on the horizontal centreline, $y = 0.5$ (solid line – the presented method, triangles – Ghia *et al.*)

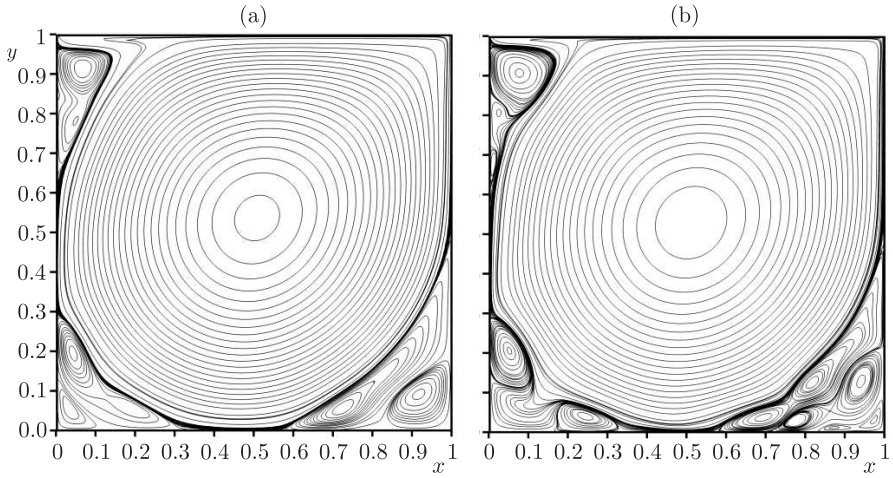

Figure 5. Square cavity – stream function contours: (a) $\mathrm{Re} = 10\,000$ on 200×200 uniform grid, (b) $\mathrm{Re} = 16\,000$ on 300×300 uniform grid

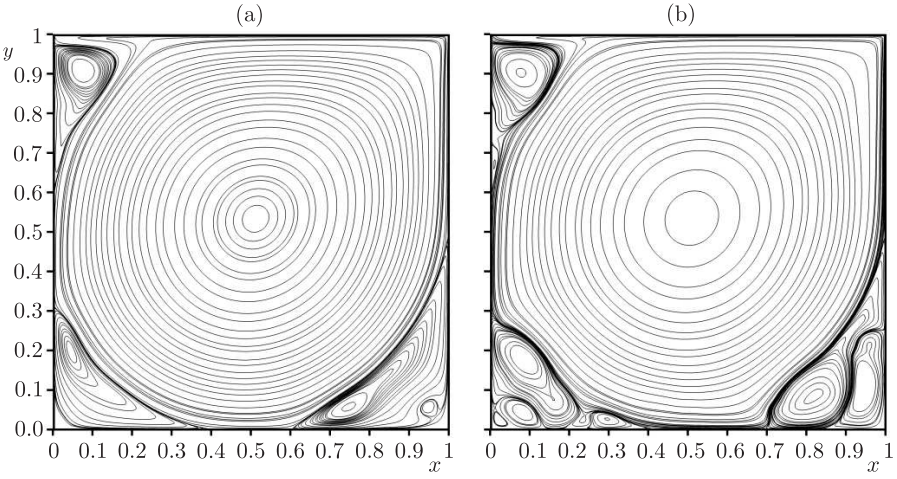

Figure 6. Square cavity – stream function contours on nonuniform 150×150 grid with $d_0 = d_N = 0.3$: (a) $\mathrm{Re} = 10\,000$, (b) $\mathrm{Re} = 16\,000$

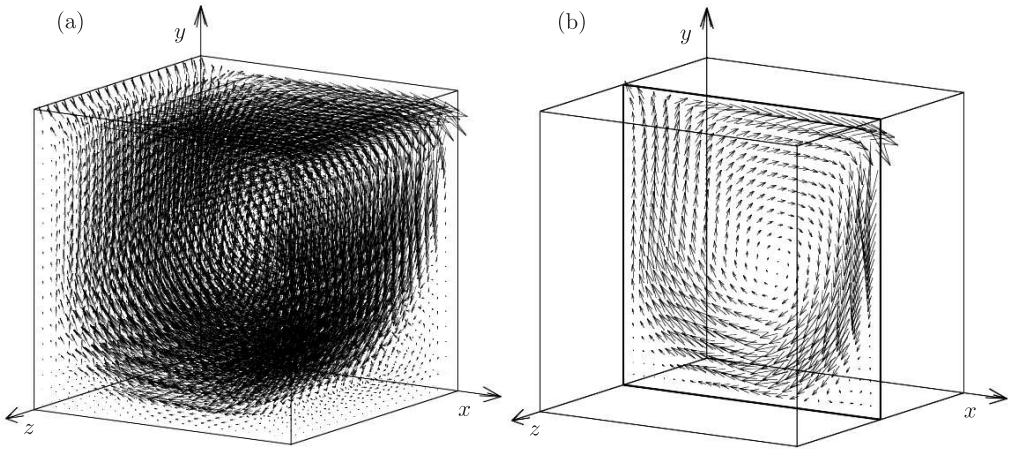

Figure 7. Cubic cavity – velocity vectors for $\mathrm{Re} = 1000$ on $100 \times 100 \times 100$ grid: (a) the whole cavity, (b) the $z = 0.5$ plane

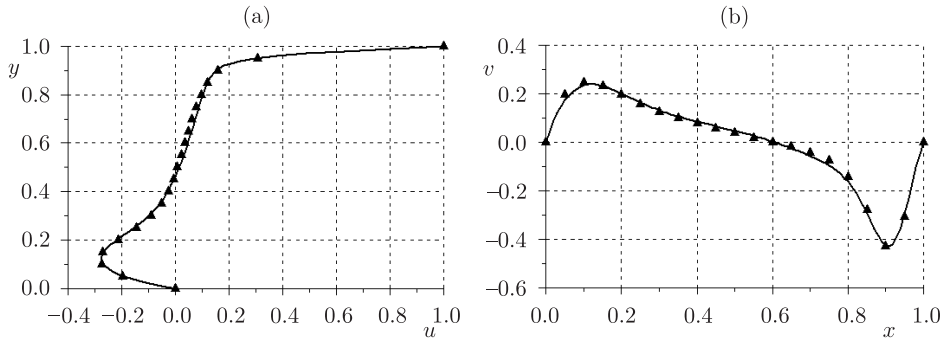

Figure 8. Cubic cavity – distributions of velocity components at $\mathrm{Re} = 1000$ on the $z = 0.5$ plane, $100 \times 100 \times 100$ grid: (a) u-velocity component on the vertical centerline, $x = 0.5$, (b) v-velocity component on the horizontal centreline, $y = 0.5$ (solid line – the presented method, triangles – Shu *et al.*)

for $\mathrm{Re} = 10\,000$ and $\mathrm{Re} = 16\,000$ on uniform and nonuniform grids are drawn in Figures 5 and 6. Taking into account that the transition from laminar to turbulent flows occurs about $\mathrm{Re} \approx 8000$ [80], the steady solutions for these Reynolds numbers are not stable and the primary vortex is still attached to the three walls of the cavity but the secondary, tertiary and successive vortices pulse slowly and reform along time. The application of unequal mesh sizes in different coordinate directions is more cost effective and the same accurate solutions can be obtained using double decreased grid sizes.

The computations for the cubic cavity problem (Figure 1b) were done on a generalised grid (10), which was generated after introducing the third spatial coordinate. A uniform $100 \times 100 \times 100$ cubical grid for $\mathrm{Re} \leq 1000$ was employed and numerical simulations were conducted with $\Delta t = 10^{-3}$. The velocity vectors of steady state solutions for the Reynolds numbers $\mathrm{Re} = 1000$ in the whole 3D cavity (Figure 7a) and on the symmetry ($z = 0.5$) plane (Figure 7b) are presented. In Figure 8, comparisons of the u-velocity profile along the vertical centreline and

v-velocity profile along the horizontal centreline of the cavity ($z = 0.5$) with the results of Shu *et al.* [91] are plotted.

4.2. Backward-facing step flow

The third case considered is the motion of a viscous liquid in a rectilinear two-dimensional backward-facing step (flow over a sudden expansion). The flow geometry is sketched in Figure 9. This simple configuration involves a few re-circulating flow regions experimentally studied by Armaly *et al.* [96]. The length of the computational domain was taken from the range $20 \leq L \leq 25$ and increased for a higher Reynolds number. At the inlet and the outlet, parabolic velocity profiles with average velocities of $u_{\text{ave}} = 1$ are assumed and no-slip conditions on solid walls are prescribed. Vanishing of the pressure derivative is postulated ($\partial p/\partial x = 0$) at the inlet and $p = 1$ is imposed at the outlet.

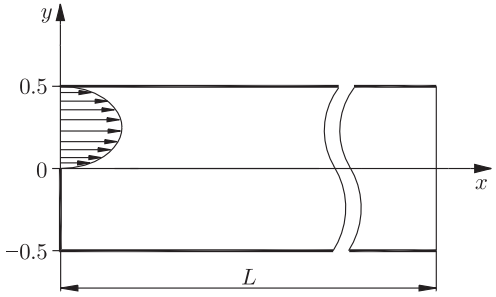

Figure 9. Geometry of backward-facing step problem

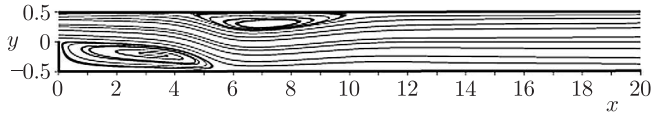

Figure 10. Backward-facing step: stream-function contours for $\text{Re} = 800$ on 1000×50 grid

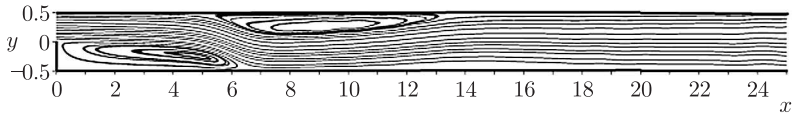

Figure 11. Backward-facing step: stream-function contours for $\text{Re} = 1200$ on 1250×50 grid

By using the developed algorithms, calculations for the backward-facing step have been performed with $10^{-2} \leq \Delta t \leq 10^{-3}$ time steps for $\text{Re} \leq 1200$ on the $50L \times 50$ uniform grids. Figures 10 and 11 give the computed stream-function contours for $\text{Re} = 800$ and $\text{Re} = 1200$ on the 1000×50 and 1250×50 uniform grids, respectively. The basic character of the backward-facing step flow at $\text{Re} = 800$ is well known and it has been established that the flow is steady up to this Reynolds number. The presented calculations have shown that the problem converges to a steady solution for critical Reynolds number $\text{Re}_{\text{kr}} \approx 1200$ and, as expected, the lengths of the separation bubbles grow with an increase in Re. The cross-channel profiles of horizontal velocity, located at $x = 7$ and $x = 15$ locations, and their comparison with those of Gartling [90] are illustrated in Figure 12.

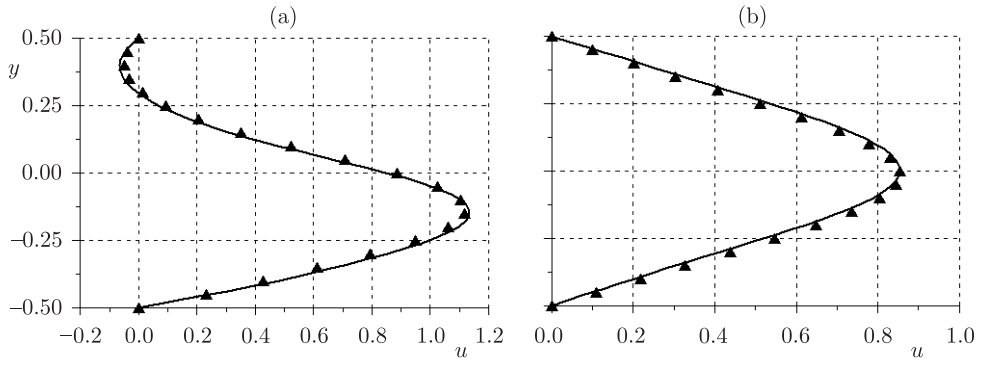

Figure 12. Backward facing step – distributions of u-velocity component at $\mathrm{Re} = 800$ on 1000×50 grid: (a) $x = 7$, (b) $x = 15$ (solid line – the presented method, triangles – Gartling)

5. Remarks and conclusions

Computational algorithms for the solution of incompressible flows of a viscous fluid, based on the velocity correction method, have been developed. The algorithms have been implemented to solve fluid flows for the classical test cases: the wind shear-driven flows in square and cubic cavities as well as the backward-facing step problem. A number of various numerical experiments have been carried out for significantly large Reynolds numbers. The comparisons between the numerical results and the results reported in numerous references show that the method is well adapted for the numerical simulations of various two- and three-dimensional problems and flows of practical interest. The algorithms are efficient when considering the computational effort involved and are applicable to computation of both laminar and turbulent motions. They have proved to be very effective for the demanded time of calculations required for computations and offer their significant acceleration in comparison with the same problem solutions obtained by using the Fluent solver. This motivates further extension of these algorithms to unsteady flows computations in geometrically complicated domains. The research in this direction is in progress. Besides, the future research can also be focused on various strategies for computation of turbulent flows.

From the above results, it is evident that a proper combination of the method of lines and relaxation-based multigrid cycles can yield fast robust solvers of high quality for the incompressible Navier-Stokes equations at high Reynolds numbers. These methods are well known powerful techniques both for the solution of time dependent partial differential equations and systems of linear algebraic equations, which are employed to discretize the Poisson equations. In particular, partial limitation of iteration numbers in conjunction with the multigrids methods and the standard Gauss-Seidel relaxation leads to very efficient computational algorithms and preserves a given accuracy.

It has been found from the grid-dependence study conducted for the mesh points distributions in spatial directions that the accuracy of numerical results for the cavities improves very quickly as the stretching of grid points increases. In particular, the calculations for square cavity flows on nonuniform grids indicate that problems can be solved on double decreased grids. Some numerical investigations have been conducted with various fourth-order finite difference approximations of spatial derivatives. These

tests leave no doubts that the second order finite-difference schemes provide the best accuracy of numerical results on the same grids in the shortest time of calculations.

References

[1] Chorin A J 1968 *Math. Comput.* **22** 745
[2] Temam R 1984 *Navier-Stokes Equations, Theory and Numerical Analysis*, Elsevier Science Pub. B. V., New York
[3] Kim J and Moin P 1985 *J. Comput. Phys.* **59** 308
[4] Hirsch Ch 1990 *Numerical Computational of Internal and External Flows. Vol 2: Computational Methods for Inviscid and Viscous Flows*, John Wiley & Sons, Chichester – New York
[5] Tanahashi T and Okanaga H 1990 *Int. J. Numer. Meth. Fluids* **11** 479
[6] Gresho P M 1990 *Int. J. Numer. Meth. Fluids* **11** 587
[7] Kovacs A and Kawahara M 1991 *Int. J. Numer. Meth. Fluids* **13** 403
[8] Karniadakis G M 1991 *J. Comput. Phys.* **97** 414
[9] Huser A D and Biringen S 1992 *Int. J. Numer. Meth. Fluids* **14** 1087
[10] Ren G and Utnes T 1993 *Int. J. Numer. Meth. Fluids* **17** 349
[11] Pinelli A and Vacca A 1994 *Int. J. Numer. Meth. Fluids* **18** 781
[12] Kosma Z 1994 *ZAMM* **74** 6
[13] Turek S 1996 *Int. J. Numer. Meth. Fluids* **22** 987
[14] Ferziger J H and Perić M 1996 *Computational Methods for Fluid Dynamics*, Springer-Verlag, Berlin – Heidelberg – New York
[15] Hugues S and Randriamampianina A 1998 *Int. J. Numer. Meth. Fluids* **28** 501
[16] Goldberg D and Ruas V 1999 *Int. J. Numer. Meth. Fluids* **30** 233
[17] Kosma Z 1999 *Determination of Laminar Incompressible Flows*, Monography of Technical University of Radom (in Polish)
[18] Guo D X 2000 *Appl. Numer. Math.* **35** 307
[19] Boivin S, Cairé F and Hérard J-M 2000 *Int. J. Therm. Sci.* **39** 806
[20] Minev P D 2001 *Int. J. Numer. Meth. Fluids* **36** 441
[21] Brown D L, Cortez R and Minion M L 2001 *J. Comput. Phys.* **168** 464
[22] Liu C H and Leung D Y C 2001 *Comput. Meth. Appl. Mech. Engrg.* **190** 4301
[23] Auteri F, Saleri F and Vigevano L 2001 *Comput. Meth. Appl. Mech. Engrg.* **190** 6927
[24] Friedrich R, Hüttl T J, Manhart M and Wagner C 2001 *Comput. Fluids.* **30** 555
[25] Christon M A 2002 *Int. J. Numer. Meth. Fluids* **38** 1177
[26] Auteri F and Parolini N 2002 *J. Comput. Phys.* **175** 1
[27] Stevens D E, Chan S T and Gresho P 2002 *Int. J. Numer. Meth. Fluids* **40** 1303
[28] Botella O 2002 *Comput. Fluids.* **31** 397
[29] Dagan A 2003 *Comput. Fluids.* **32** 1213
[30] Guermond J L and Shen J 2003 *J. Comput. Phys.* **192** 262
[31] Grauer R and Spanier F 2003 *J. Comput. Phys.* **192** 727
[32] Kosma Z 2003 *Numerical Simulation of Viscous Fluid Motions*, Monography of Technical University of Radom (in Polish)
[33] Manhart A 2004 *Comput. Fluids.* **33** 435
[34] Fernandez-Feria R and Sanmiguel-Rojas E 2004 *Comput. Fluids.* **33** 463
[35] Löhner R 2004 *J. Comput. Phys.* **195** 143
[36] Minion M L 2004 *Appl. Numer. Math.* **48** 369
[37] Blasco J and Codina R 2004 *Appl. Numer. Math.* **51** 1
[38] Liu M, Ren Y-X and Zhang H 2004 *J. Comput. Phys.* **200** 325
[39] Guy R D and Fogelson A L 2005 *J. Comput. Phys.* **203** 517
[40] Abide S and Viazzo S 2005 *J. Comput. Phys.* **206** 252
[41] Albensoeder S and Kuhlmann H C 2005 *J. Comput. Phys.* **206** 536
[42] Li X and Han X 2005 *Int. J. Numer. Meth. Fluids* **49** 395
[43] Bejanov B, Guermond J-L and Minev P D 2005 *Int. J. Numer. Meth. Fluids* **49** 549
[44] Kosma Z 2005 *TASK Quart.* **9** (1) 37

[45] Wong J C-F and Chan M K-H 2006 *Int. J. Numer. Meth. Fluids* **51** 385
[46] Gervasio P, Saleri F and Veneziani A 2006 *J. Comput. Phys.* **214** 347
[47] Jobelin M, Lapuerta C, Latché J-C, Angot P and Piar B 2006 *J. Comput. Phys.* **217** 502
[48] Zheng Z and Petzold L 2006 *J. Comput. Phys.* **219** 976
[49] Codina R and Badia S 2006 *Comput. Meth. Appl. Mech. Engrg.* **195** 2900
[50] Löhner R, Yang C, Cebral J, Camelli F, Soto O and Waltz J 2006 *Comput. Meth. Appl. Mech. Engrg.* **195** 3087
[51] Kress W and Lötstedt P 2006 *Comput. Meth. Appl. Mech. Engrg.* **195** 4033
[52] Guermond J L, Minev P and Shen J 2006 *Comput. Meth. Appl. Mech. Engrg.* **195** 6011
[53] Aprivitola A and Denaro F M 2007 *Int. J. Numer. Meth. Fluids* **53** 1127
[54] Jan Y-J and Sheu T W-H 2007 *Comput. Meth. Appl. Mech. Engrg.* **196** 4755
[55] Pontaza J P 2007 *J. Comput. Phys.* **225** 1590
[56] Utnes T 2008 *J. Comput. Phys.* **227** 2198
[57] Kosma Z 2008 *Numerical Methods for Engineering Applications, 5-th Edition*, Technical University of Radom Publishing (in Polish)
[58] Ghia U, Ghia K N and Shin C T 1982 *J. Comput. Phys.* **48** 387
[59] Kim J and Moin P 1985 *J. Comput. Phys.* **59** 308
[60] Tanahashi T and Okanaga H 1990 *Int. J. Numer. Meth. Fluids* **11** 479
[61] Kovacs A and Kawahara M 1991 *Int. J. Numer. Meth. Fluids* **13** 403
[62] Ren G and Utnes T 1993 *Int. J. Numer. Meth. Fluids* **17** 349
[63] Li M, Tang T and Fornberg B 1995 *Int. J. Numer. Meth. Fluids* **20** 1137
[64] Barragy E and Carey G F 1997 *Comput. Fluids* **26** 453
[65] Botella O and Peyret R 1998 *Comput. Fluids* **27** 421
[66] Shankar P N and Deshpande M D 2000 *Annu. Rev. Fluid Mech.* **32** 93
[67] Aydin M and Fenner R T 2001 *Int. J. Numer. Meth. Fluids* **37** 45
[68] Barton I E, Markham-Smith D and Bressloff N 2002 *Int. J. Numer. Meth. Fluids* **38** 747
[69] Peng Y-F, Shiau Y-H and Hwang R R 2003 *Comput. Fluids* **32** 337
[70] Mai-Duy N and Tran-Cong T 2003 *Int. J. Numer. Meth. Fluids* **41** 743
[71] Sahin M and Owens R G 2003 *Int. J. Numer. Meth. Fluids* **42** 57
[72] Sahin M and Owens R G 2003 *Int. J. Numer. Meth. Fluids* **42** 79
[73] Piller M and Stalio E 2004 *J. Comput. Phys.* **197** 299
[74] Gravemeier V, Wall W A and Ramm E 2004 *Comput. Meth. Appl. Mech. Engrg.* **193** 1323
[75] Ramšak M and Škerget L 2004 *Int. J. Numer. Meth. Fluids* **46** 815
[76] Wu Y and Liao S 2005 *Int. J. Numer. Meth. Fluids* **47** 185
[77] Erturk E, Corke T C and Gökçöl C 2005 *Int. J. Numer. Meth. Fluids* **48** 747
[78] Brüger A, Gustafsson B, Lötstedt P and Nilsson J 2005 *J. Comput. Phys.* **203** 49
[79] Abide S and Viazzo S 2005 *J. Comput. Phys.* **206** 252
[80] Gelhard T, Lube G, Olshanskii M A and Starcke J-H S 2005 *J. Comput. Appl. Math.* **177** 243
[81] Bruneau C-H and Saad M 2006 *Comput. Fluids* **35** 326
[82] Masud A and Khurram R A 2006 *Comput. Meth. Appl. Mech. Engrg.* **195** 1750
[83] Prabhakar V and Reddy J N 2006 *J. Comput. Phys.* **215** 274
[84] Guy G and Stella F 1993 *J. Comput. Phys.* **106** 286
[85] Jiang B-N, Lin T L and Povinelli L A 1994 *Comput. Meth. Appl. Mech. Engrg.* **114** 213
[86] Tang L Q, Cheng T and Tsang T T H 1995 *Int. J. Numer. Meth. Fluids* **21** 413
[87] Dridakis D, Iliev O P and Vassileva D P 1998 *J. Comput. Phys.* **146** 301
[88] Paisley M F 1999 *Int. J. Numer. Meth. Fluids* **30** 441
[89] Liu C H 2001 *Int. J. Numer. Meth. Fluids* **35** 533
[90] Sheu T W H and Tsai S F 2002 *Comput. Fluids* **31** 911
[91] Shu C, Wang L and Chew Y T 2003 *Int. J. Numer. Meth. Fluids* **43** 345
[92] Nithiarasu P, Mathur J S, Weatherill N P and Morgan K 2004 *Int. J. Numer. Meth. Fluids* **44** 1207
[93] Lo D C, Murugesan K and Young D L 2005 *Int. J. Numer. Meth. Fluids* **47** 1469
[94] Albensoeder S and Kuhlmann H C 2005 *J. Comput. Phys.* **206** 536

[95] Ding H, Shu C, Yeo K S and Xu D 2006 *Comput. Meth. Appl. Mech. Engrg.* **195** 516
[96] Armaly B F, Durst F, Pereira J C F and Schönung B 1983 *J. Fluid Mech.* **127** 476
[97] Gartling D K 1990 *Int. J. Numer. Meth. Fluids* **11** 953
[98] Pentaris A, Nikolados K and Tsangaris S 1994 *Int. J. Numer. Meth. Fluids* **19** 1053
[99] Pappou T and Tsangaris S 1997 *Int. J. Numer. Meth. Fluids* **25** 523
[100] Barton I E 1997 *Int. J. Numer. Meth. Fluids* **25** 633
[101] Barton I E 1998 *Int. J. Numer. Meth. Fluids* **28** 841
[102] Keskar J and Lyn D A 1999 *Int. J. Numer. Meth. Fluids* **29** 411
[103] Domański J J and Kosma Z 2001 *ZAMM* **81** (S4) 921
[104] Pontaza J P and Reddy J N 2003 *J. Comput. Phys.* **190** 523
[105] Fernandez-Feria R and Sanmiguel-Rojas E 2004 *Comput. Fluids* **33** 463
[106] Liu M, Ren Y-X and Zhang H 2004 *J. Comput. Phys.* **200** 325
[107] Ramšak M, Škerget L, Hriberšek M and Žunič Z 2005 *Eng. Anal. Bound. Elem.* **29** 1
[108] Kosma Z 2005 *TASK Quart.* **9** (1) 17
[109] Pontaza J P 2006 *J. Comput. Phys.* **217** 563